Numerical Modeling of Helical External Gear Pump Through a Novel CFD Approach Using Simerics MP+

Pietro Mazzei[1], Emma Frosina[2], Simone Bulleri[3], Adolfo Senatore[1].

[1]Department of Industrial Engineering, University of Naples Federico II, Via Claudio, 21, 80125 Naples, Italy, pietro.mazzei2@unina.it (P.M.), senatore@unina.it (A.S.).

[2]Department of Engineering, University of Sannio, Piazza Roma, 21, 82100 Benevento, Italy, frosina@unisannio.it.

[3]Research Department, Hydreco Hydraulics Italia, Vignola, Modena, Italy, sbulleri@hydreco.com

Abstract.

External Gear Pumps (EGPs) are positive displacement machines with excellent performances and very competitive costs. A particular typology of EGPs is Helical Gear Pump, where the teeth present an inclination along the axial direction, permitting a progressive meshing with consequent lower vibration and noise emission.
Three-dimensional CFD numerical analysis of these pumps has proven to be quite complex. More recently some analyses have been proposed however, to obtain realistic results, approximations regarding the helical angle along the axial dimension have been applied. Those models consisted of a high number of grid cells, leading to high computational time request. In this article, it is explored the use of a novel CFD approach through the use of the commercial code Simerics MP+, already used with success by the research group. This new method permits to evaluate the geometry of the pump without any geometrical approximation, leading to more accurate results and less computational time required if compared with other 3D-CFD tools. An accurate numerical model has been built up on a reference pump with helical gears; the model has been then compared with the results of an experimental campaign.
Finally, a new design of the pressure relief grooves inside the wear plates has been investigated and simulated with the objective of reducing the fluid-borne noise emission, as well as to improve the volumetric efficiency of the pump and to reduce the flow ripple fluctuation, pressure spikes and crossflow optimization.

Keywords. Helical EGPs, Helical Gears, 3D CFD modelling, flow ripple, fluid-borne noise, design optimization.

1. INTRODUCTION

Helical external gears pumps (EGPs) are a type of positive displacement machines that have similar volumetric performances of traditional spur gears EGPs while producing less vibrations and lower noise emissions thanks to the more progressive meshing permitted by their geometry design. The same design sets some additional challenges respect to traditional spur gear, though. The particular gear design generates a variable axial force during the meshing that make the design of the balancing surfaces of the wear plates more demanding.

The desire to harness these advantages have pushed the scientific community to search ways to better understand and accurately simulate this EGP typology. One way to simulate the working condition is through the use of a three-dimensional CFD numerical modeling. The three-dimensional CFD numerical modeling of helical gears pumps has always proven to be a challenging matter due to the difficulty in following the helical angle along the axial direction that requires the implementation of a number of geometry approximation.

Until recent times, the only way to simulate those pumps through a three-dimensional CFD analysis was to slice up the gears along the axial direction and treat every slice as spur gears in connection to the adjacent slices. This methodology allows to obtain a good accuracy, as it can be seen in other similar works found in scientific literature [1,2], but require a high number of grid cells and mismatched grid interface with consequent higher computational time.

In this paper, a novel three-dimensional CFD approach has been applied by using a new capability available in the commercial code Simerics MP+, developed by Simerics Inc. This approach implements the use of a body-fitted binary tree grid generator that accurately follows the fluid volume extracted along the gears' helical angle. The parent-child tree architecture permits to obtain expandable data structure with reduced memory storage, generating thus an accurate and efficient grid, hence eliminating the needs of geometry approximations.

This novel approach has then been validated through experimental tests performed on a test rig of Duplomatic MS Group. After this validation process, a new design of the pressure relief grooves inside the wear plate has been investigated with the objective of improving the volumetric efficiency while reducing the flow ripple fluctuation.

2. PUMP ANALYZED AND EXPERIMENTAL TEST SETUP

The new mentioned numerical methodology has been applied on a reference external helical gear pump produced by Hydreco Hydraulics Italia with a displacement of 14.5 cm3/rev.

The basic technical data of the pump are listed in Table 1.

The pump has a housing made from die-cast alloy, making it ideal for mobile application. An assembly vision of the pump is visible in Figure 2.1. a); while in Figure 2.1. b) there is the exploded view.

Table 1. PUMP TECHNICAL DATA

Description	*Value*	*Unit*
Nominal displacement	14.5	cm^3/rev
Max. continuous pressure	260	bar
Max. intermitted pressure	290	bar
Max. peak pressure	310	bar
Min. rotational speed	500	rev/min
Max. rotational speed	3500	rev/min

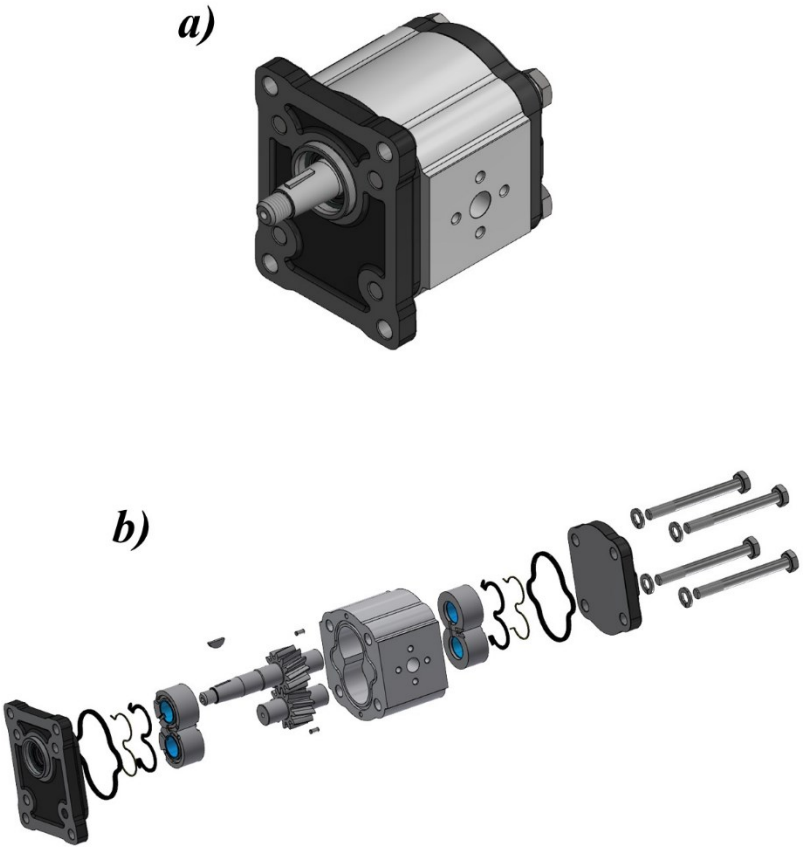

Figure 2.1. a) Assembly of the reference helical gears pump; b) Exploded view

The experimental campaign to validate the model has been executed on a dedicated test bench at Duplomatic MS. The test bench layout is shown in Figure **2.2**. There are two strain gauge sensors, P1 at the inlet side (Duplomatic model PTH, scale: -1÷10 bar and ±0.25% FS) and P2 at the delivery side (Duplomatic model PTH, scale: 0÷400 bar and ±0.25% FS). The flow-rate meter Q1 is a VSE VS 0.4 (VSE.flow®, Neuenrade, Germany), scale 0.03÷40 L/min, 0.3% measured value accuracy.

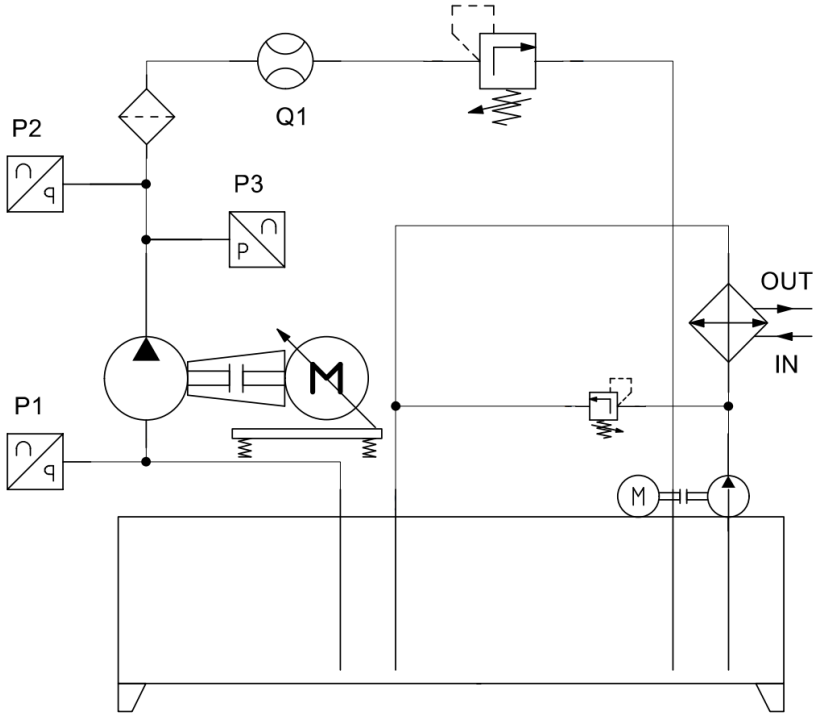

Figure 2.2. Test bench layout

The tests have been carried out with an oil ISO 46, grade HL, maintained at a temperature of 40° C ± 1°C. The pump has been tested varying the delivery pressure at different fixed speeds.

Pressure ripples have been also acquired by adding a fixed orifice after the P2 strain gauge sensors to impose the load and a P3 high frequency pressure sensor (PCB® model 113B26, PCB Piezotronics, Inc.,NY, USA) between the tested pump and the P2 strain gauge.

The experimental campaign has involved the analysis of a numbers of working conditions with the additional measurement of the noise levels. Being the numerical model focused on the fluid dynamic aspect, only some of the experimental data has been compared to the results obtained from the numerical model, as shown in section 4.

3. THE THREE-DIMENSIONAL CFD NUMERICAL MODEL

3.1. Numerical Model Description

The numerical model has been developed using the commercial code Simerics MP+®, developed by Simerics Inc. This tool has been specifically designed to analyze hydraulic components, offering a variety of templates for specific case of pumps, motors and valves.

The pump fluid domain utilized has been extracted from the CAD files of the pump, as it can be seen in Figure 3.1.

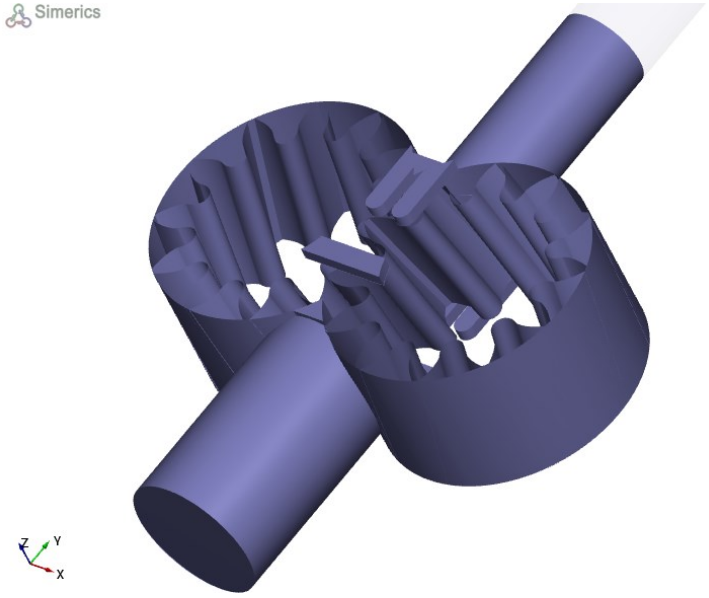

Figure 3.1. Helical pump fluid domain

It has been meshed using a body-fitted binary tree approach with the use of the rotor template Mesher to implement the rotation of the helical gears. An analysis with coarser and finer mesh has also been explored; the results obtained from the first ones have proved to have too low accuracy, while the latter have a precision increase such that it is not justified by the higher computational power and time required to reach the converge of the solution.

The final model with the selected grid contains around 950,000 cells and it is shown in Figure 3.2.

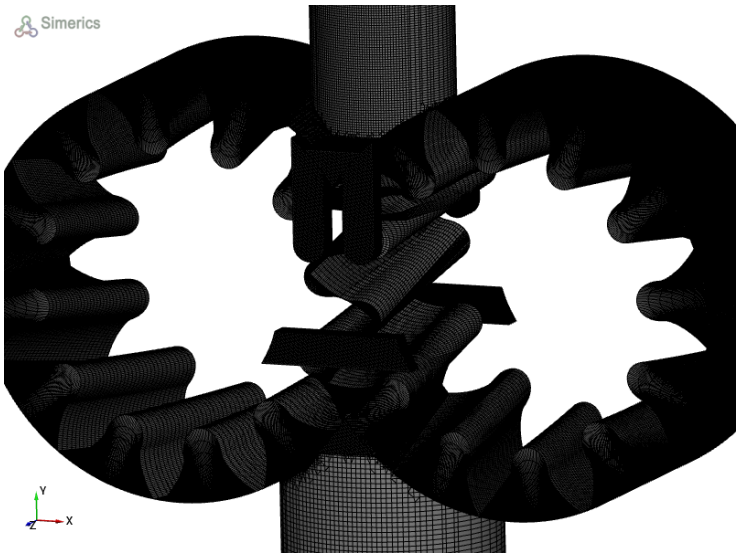

Figure 3.2. Mesh grid of pump's fluid domain

The simulations have been run on a workstation equipped with an Intel® Xeon® CPU E5-2640v2 @ 2.00 GHz (two processors) with 192 GB RAM. The computational time required to complete a simulation with an angular step size of 0.5 degree of gear shaft rotation is about 72 hours for two pump revolutions.

The gears in the model have been translated along the vertical axis to consider the effect of the pressure forces acting on the gears. The driven gear has also been rotated to reproduce the contact with the Driving gear. The numerical simulation does not permit to evaluate a zero gap, so the choice of the minimal value of the gap is of utmost importance to replicate real working conditions.

A value of 27 µm has been initially selected for the gap between the teeth and the one between the teeth and the housing. This initial value led to unrealistic crossflow values during the meshing. Thus, a more restrictive value of 5 µm has been chosen as minimal gap value, as shown in Figure 3.3. This resulted in an increase of the cell required to reach a stable solution.

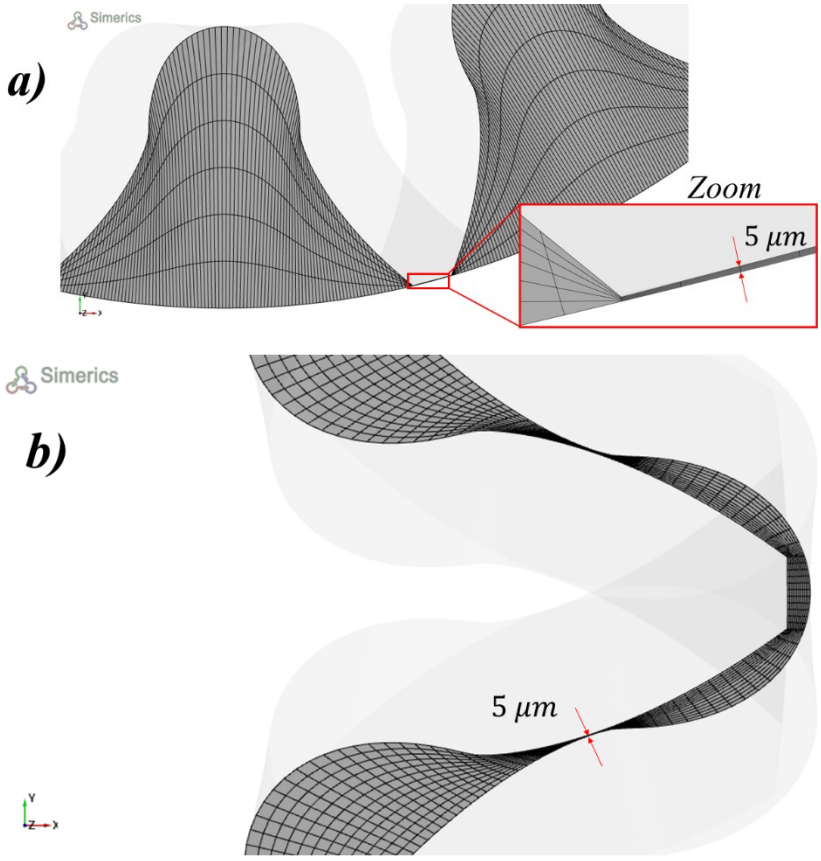

Figure 3.3. a) Minimum size gap housing-tooth contact; b) minimum size gap meshing teeth contact

The numerical model includes the evaluations of turbulence and cavitation. The turbulence has been predicted by the use of a standard k-ε turbulence model. Despite the presence in the literature of more accurate model than the k-ε, for this application where the losses due to the viscous stresses are negligible compared to pressure forces, this model permits to obtain a good accuracy requiring only a minimal amount of additional computational power. The reliability of this methodology implemented can be seen in numerous works available in literature [3-7].

3.2. Cavitation Model Description

The cavitation model utilized is directly available in the code and is able to predict cavitating conditions with high accuracy. It is built on the work of Singhal et al., based on the Rayleigh-Plesset equation [6] and appraises for cavitation, aeration and liquid compressibility. This model describes the vapor distribution using the following formulation:

$$\frac{\partial}{\partial t}\int_{\Omega(t)} \rho\, f_v d\Omega + \int_{\sigma} \rho\big((\vec{v} - \overrightarrow{v_\sigma}) \cdot \vec{n}\big) f_v d\sigma = \int_{\sigma} \left(D_f + \frac{\mu_t}{\sigma_f}\right)(\nabla f_v \cdot \vec{n}) d\sigma + \int_{\Omega} (R_e - R_c) d\Omega \tag{3.1}$$

Where D_f is the diffusivity of the vapor mass fraction and σ_f is the turbulent Schmidt number. In the following study, these two numbers are set equal to the mixture viscosity and unity, respectively. The vapor generation term, R_e, and the condensation rate, R_c, are characterized as:

$$R_e = C_e \frac{\sqrt{k}}{\sigma_l} \rho_l \rho_v \left[\frac{2}{3}\frac{(p - p_v)}{\rho_l}\right]^{\frac{1}{2}} \left(1 - f_v - f_g\right) \tag{3.2}$$

$$R_c = C_c \frac{\sqrt{k}}{\sigma_l} \rho_l \rho_v \left[\frac{2}{3}\frac{(p - p_v)}{\rho_l}\right]^{\frac{1}{2}} f_v \tag{3.3}$$

The Singhal's cavitation theory has been extended to also include non-condensable gases (NCG) in the liquid [7]. The unsteady mixture (liquid, liquid vapor and NCG) density ρ is evaluated in according to the equation (3.4):

$$\frac{1}{\rho} = \frac{f_v}{\rho_v} + \frac{f_g}{\rho_g} + \frac{(1 - f_v - f_g)}{\rho_l} \tag{3.4}$$

The NCG in the hydraulic fluid can be found as a free and a dissolved state. The model utilized for this activity implement an Equilibrium Dissolved Gas Model approach, which assumes that the free NCG mass fraction is not constant. Its evaluation is obtained by the resolutions of an additional transport equation for the mass fraction of the dissolved gas (3.5).

$$\frac{\partial}{\partial t}\int_{\Omega(t)} \rho\, f_d d\Omega + \int_{\sigma} \rho\left(\left(\left(\vec{v} - \overrightarrow{v_\sigma}\right)\cdot\vec{n}\right) f_d d\sigma\right) = \int_{\sigma}\left(D_{f_d} + \frac{\mu_t}{\sigma_f}\right)(\nabla f_d \cdot \vec{n}) d\sigma \int_{\Omega} \frac{\rho\left(f_d - f_{d,equil}\right)}{\tau} d\Omega + \int_{\Omega}\left(S_{f_d}\right) d\Omega \quad (3.5)$$

Where the equilibrium gas mass fraction $f_{d,equil}$ depends on the active cell pressure and is evaluated through the following equation:

$$f_{d,equil} = \frac{p}{p_{f_{d,equil\,ref}}} \cdot f_{d,equil\,ref} \quad (3.6)$$

Hereby, the NCG_{tot}, sum of the free gas mass fraction and the dissolved gas mass fraction is constant:

$$NCG_{tot} = f_g + f_d \; = const. \quad (3.7)$$

Under these assumptions, only one equation must be resolved for the dissolved gas f_d; the free gas f_g is subsequently evaluated based on the assumption of the NCG_{tot} being constant.

4. MODEL VALIDATION

The experimental tests have been conducted on the test bench described previously. The pump has been tested under four different pump speeds: 1000, 1500, 1800 and 2200 rev/min. The values of the delivery flow rate have been for all the delivery pressure conditions in the range of 20÷240 bar.

Due to the high computational time required to complete a simulation, only two discrete single delivery pressure points for three different pump speeds have been completely simulated. In detail, the simulations have been run at a delivery pressure of 100 bar and 200 bar with a pump speed of 1000 and 1500 rev/min. In Figure 4.1 is shown a comparison between the numerical model and the experimental results for the delivery flow-rate values (normalized to reference value, Q_{ref}) of the reference pump.

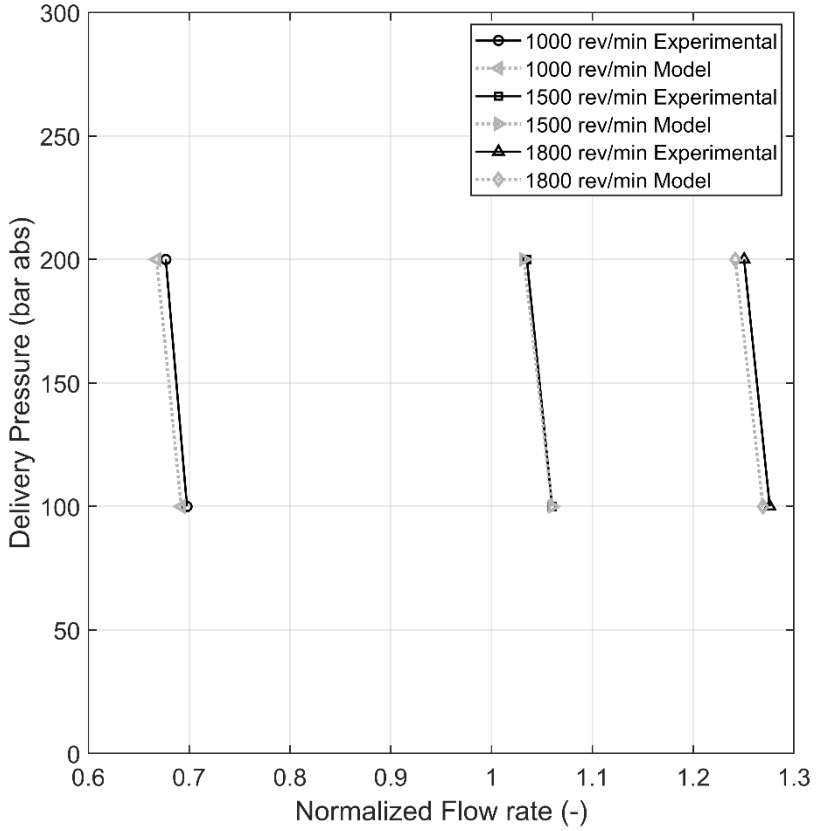

Figure 4.1. Pressure vs. normalized delivery flow rate comparison at different pump speed: 1000 rev/min, 1500 rev/min and 1800 rev/min

It can be noted that the numerical model correctly predicts the flow-rate trends for all the simulated pump speeds; the error percentage between model and experimental data is always below 1%, staying thus within the uncertainty range of the experimental measurements.

A study of the pressure ripple at the delivery side of the pump has been also conduced to further validate the numerical model. To reproduce the same conditions of the experimental campaign, the numerical model has been modified introducing a duct and an orifice both shown in Figure 4.2.

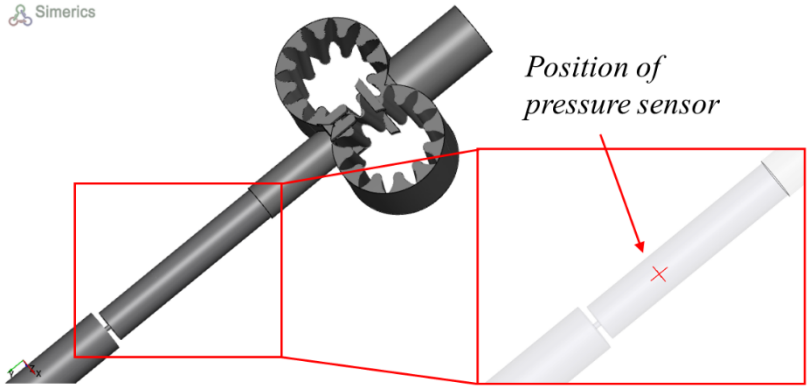

Figure 4.2. Pressure ripple analysis: Fixed orifice and the monitoring point

The comparison between model and experimental data are presented in Figure 4.3 for a single working condition. The pressure ripple values are normalized against a pressure reference value, p_{ref}. The chart reveals that there is good accordance between the experimental data and the results obtained from the numerical model. The small disagreement presents on the peaks of the pressure ripples is most likely due to the presence of high frequency noise in the experimental measurements due to the test bench setup not been perfectly isolated.

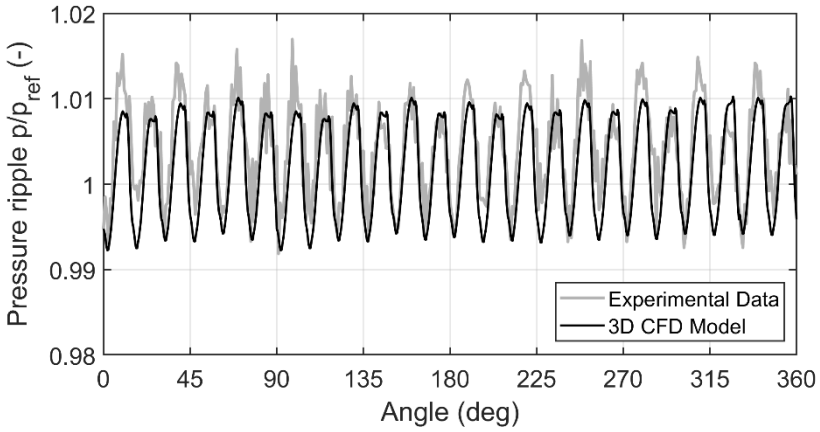

Figure 4.3. Normalize pressure ripples comparison at n=1500 rev/min

The performed comparisons have permitted to verify the high accuracy of the developed 3D numerical model for both steady-state and transient output parameters.

5. PUMP DESIGN OPTIMIZATION INVESTIGATION

After the process of validating the numerical model, a new design of the pressure relief grooves in the wear plate has been investigated. The relief grooves act as noise reducers by realizing a gradual switch between the displacing chambers and their connections with the outlet and inlet ports, thereby limiting pressure spikes and flow ripple fluctuations but also

generating an undesirable cross-flow between the suction and the delivery volumes. The new design proposed has the objective to improve the volumetric efficiency while reducing the fluid-borne noise emissions.

This new design has been developed with the idea of exploiting the offset angle between front and rear gears' faces due to the helical angle, implementing thus an asymmetrical design. This is in contrast with the current design, which presents a symmetrical geometry between the front and the rear for lean production and assembly reasons (Figure 5.1 a).

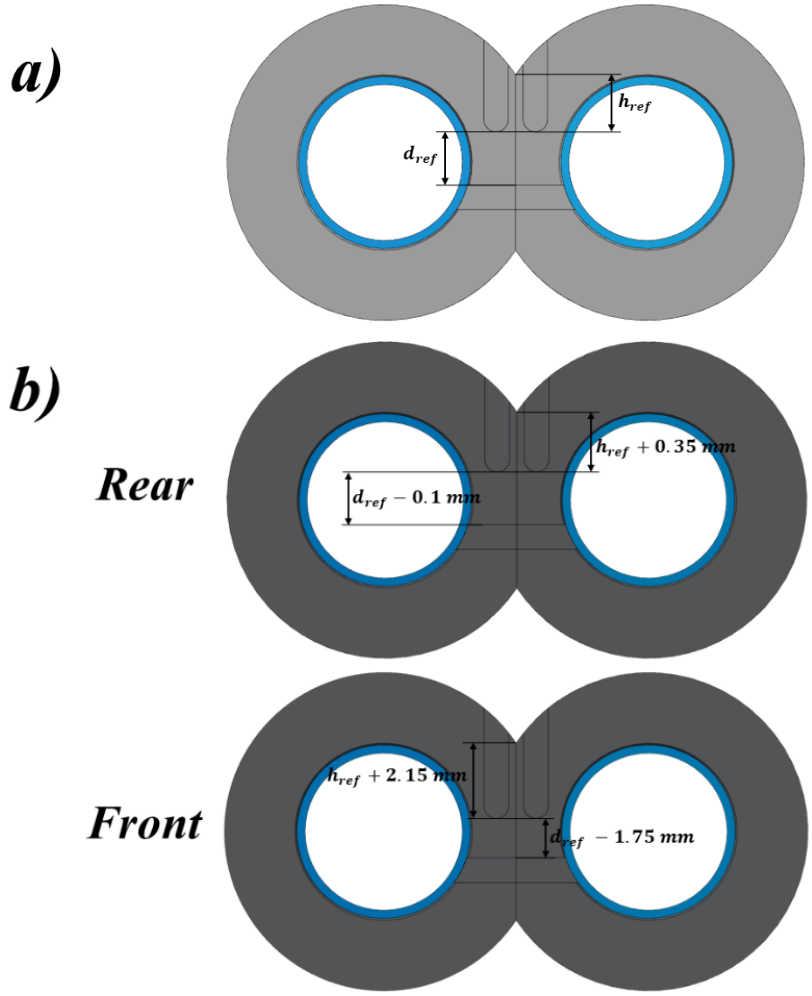

Figure 5.1. a) Relief grooves design of the standard pump; b) Proposed new design of the relief grooves

The asymmetrical design allows to control the pump timings through the length of the delivery relief grooves of the rear face and the position of the suction relief groove of the front face. This permits increased freedom for the remaining relief grooves; their length and position could then be chosen to improve the volumetric efficiency, to reduce pressure spikes and flow ripple fluctuations or a mix of both effects. The final geometry tested is shown in Figure 5.1. b).

The preliminary nature of the investigation coupled with the high computational time required to run a simulation has led to the complete simulation of this new pump design geometry for only one pump speed, 1500 rev/min, and one delivery pressure, 200 bar.

The results comparison between the standard design and the new prototyped design for the same test condition are shown in Figure 5.2 and in Table 2, where the numerical flow ripple and the numerical mean flow rate comparisons are presented with values normalized to a reference value, Q_{ref}.

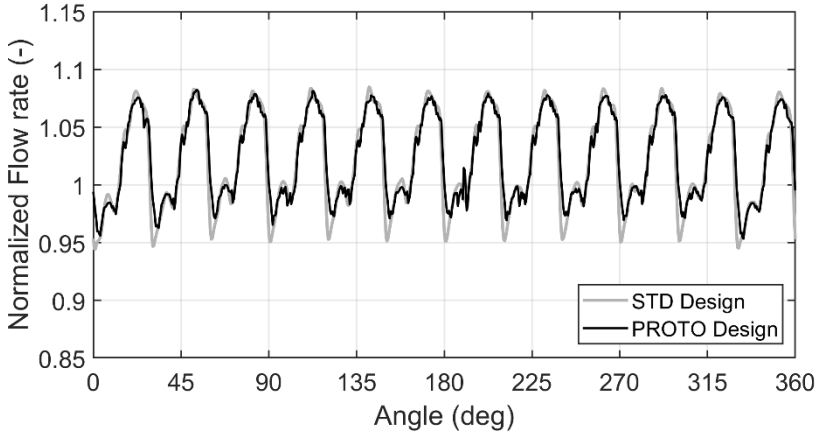

Figure 5.2. Numerical flow ripple comparison at n=1500 rev/min, Δp=200 barA

Table 2. RELIEF GROOVES DESIGN COMPARISON N=1500 REV/MIN ΔP=200 BARA

Description	***Value***	***Unit***
Mean flow rate STD Design	1.021	Q_{ref}
Mean flow rate PROTO Design	1.024	Q_{ref}

It can be appreciated from the table that the new design has a small advantage regarding the mean delivery flow, exhibiting a value increase of about 0.5%, pointing the way to a small improvement of the volumetric efficiency.

The analysis of Figure 5.2 reveals that the new investigated design permits to reduce the flow ripple, with a significant reduction of the crossflow rate. The non-uniformity rate of the

flow ripple is reduced of around 8%, confirming the increment of the average delivery flow rate. Another significative result is presented in Figure 5.3 where it is shown the comparison of the pressure evolution inside a chamber in rotation for each gear for the two tested designs. In particular, Figure 5.3. a) refers to a chamber of the driving gear, while the Figure 5.3. b) corresponds to one of the driven gear.

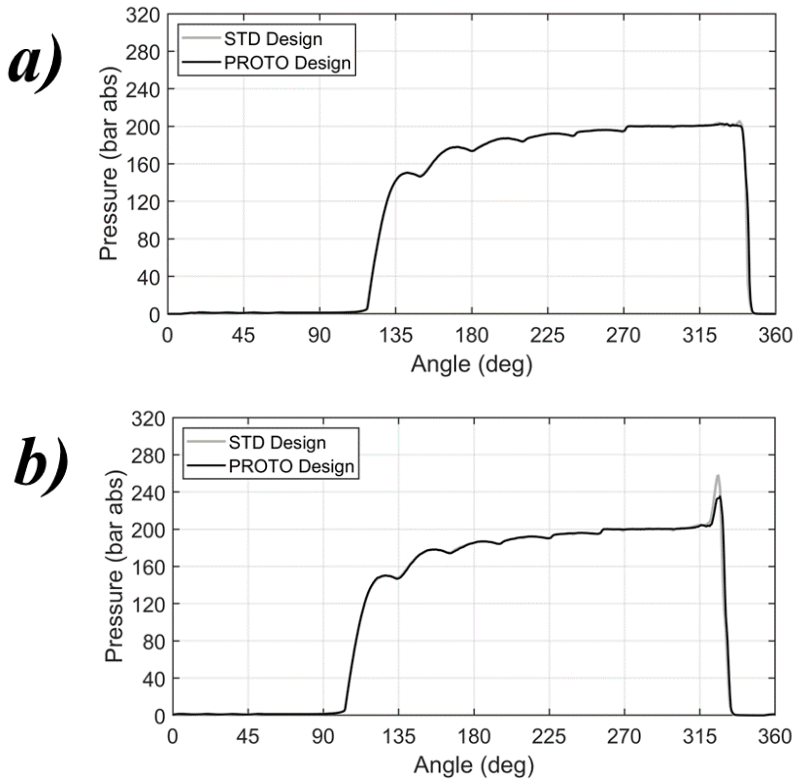

Figure 5.3. Numerical pressure evolutions comparison at n=1500 rev/min, Δp=200 barA: a) driving gear; b) driven gear.

Pressure spikes visible in Figure 5.3 are zoomed in Figure 5.4. a) and Figure 5.4. b). In particular, Figure 5.4. a) presents the zoomed view of the pressure spikes that occurs during meshing inside a chamber of the driving gear, while Figure 5.4. b) is the corresponding view in a chamber of the for the driven gear.

The examination of these results shows that the new proposed design presents lower pressure spikes during gears' meshing inside the chambers for both driving and driven gears. These results, coupled with the reduction of the non-uniformity rate of the flow ripple, suggest that the new design of the pressure relief grooves in the wear plate could provide reduction in the vibrations produced hence diminished noise emissions.

It is expected that for higher rotational speeds the pressure peaks inside a chamber during meshing will be more intense, so the advantages shown by the new proposed design could

be more relevant. For this reason, a simulation at 1800 rev/min has been executed on both new proposed design and the standard design.

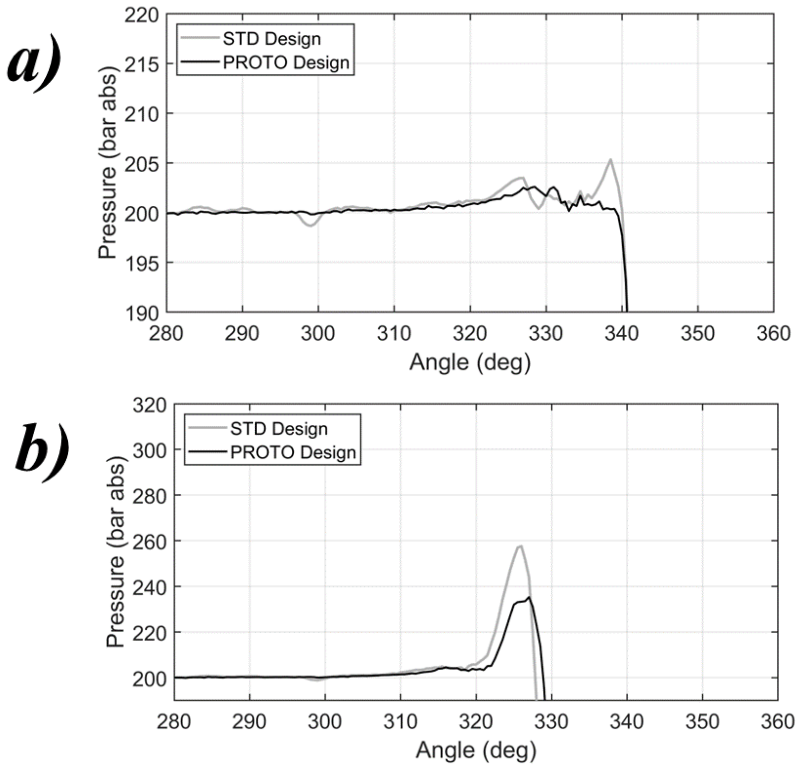

Figure 5.4. Zoomed view of numerical pressure evolutions comparison at n=1500 rev/min, Δp=200 barA: a) driving gear; b) driven gear.

The results obtained are reported in Figure 5.5 and Table 3, where the numerical flow ripple and the numerical mean flow rate comparisons are presented with values normalized to a reference value, Q_{ref}.

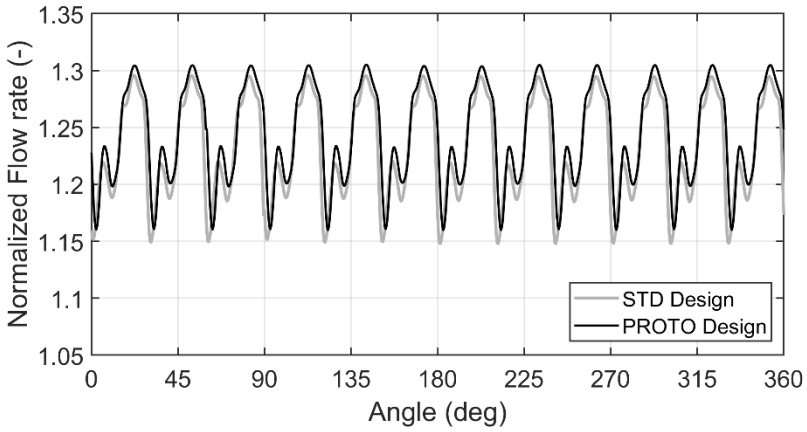

Figure 5.5. Numerical flow ripple comparison at n=1800 rev/min, Δp=200 barA

In Figure 5.6 a zoomed view of the pressure evolution inside a chamber in rotation for each gear in the meshing zone is presented for the two tested designs.

Table 3. RELIEF GROOVES DESIGN COMPARISON N=1800 REV/MIN ΔP=200 BARA

Description	***Value***	***Unit***
Mean flow rate STD Design	1.231	Q_{ref}
Mean flow rate PROTO Design	1.247	Q_{ref}

The analysis of Figure 5.5 and Table 3 demonstrate that for a higher angular speed the new design continues to improve the volumetric efficiency and the non-uniformity rate, albeit in a lesser percentage.

The investigation of Figure 5.6 shows that the pressure spikes are again less intense than the standard design, with a percentage difference more conspicuous, hence confirming the expected hypothesis.

Thus, to reach a conclusive evaluation regarding this new proposed design, it is necessary to simulate and analyze other pump working conditions to discover if this improved behavior appears as well or if it is only an isolate case of the specific pump working condition simulated.

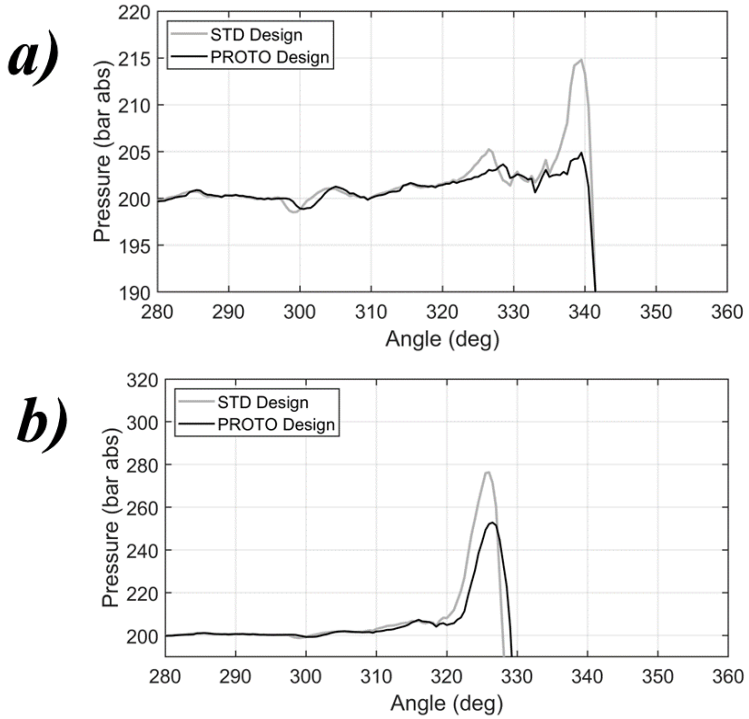

Figure 5.6. Zoomed view of numerical pressure evolutions comparison at n=1800 rev/min, Δp=200 barA: a) driving gear; b) driven gear

6. CONCLUSIONS

A novel three-dimensional CFD approach for the study of an external helical gear pump has been described in this article. This approach has been used to develop a numerical model using the commercial code Simerics MP+®, developed by Simerics Inc. The model has been realized based on a geometry of a reference pump manufactured by Hydreco Hydraulics Italia and include accurate tools to predict flow-rate, turbulence and cavitation.

An experimental test campaign, to compare and validate the results of the developed model, has been carried out on a dedicated test bench on the pump used as reference. The comparison has proved good agreement between model and experimental data under a number of working conditions, demonstrating the accuracy of the simulated model. Therefore, the approach can be used to study and optimize design of External helical gear pump.

For this reason, the approach has been applied studying a new design of the geometry of the pressure relief grooves. The results obtained from this first analysis has given interesting results and represent the first step for a further geometry optimization.

ACKNOWLEDGMENT

The authors would like to thank Simerics Inc. for providing them Simerics MP+® licenses. The authors appreciate the technical support from Roberto Maddalon of Duplomatic MS and Simone Bulleri from Hydreco Hydraulics Italia.

NOMENCLATURE

Acronym	*Description*
EGP	External Gear Pump
CFD	Computational Fluid Dynamic
CAD	Computer Aided Drafting
NCG	Non-Condensable Gas

Symbol	*Description*	*Unit*
C_c	Cavitation Condensation coefficient	[-]
C_e	Cavitation Evaporation coefficient	[-]
D_f	Diffusivity of the vapor mass fraction	[m^2/s]
D_{f_d}	Diffusivity of the dissolved NCG	[m^2/s]
f_g	Mass fraction of free NCG	[-]
f_d	Mass fraction of dissolved NCG	[-]
$f_{d,equil}$	Equilibrium gas mass fraction of dissolved NCG	[-]
$f_{d,equil\,ref}$	Equilibrium mass fraction of the dissolved NCG at the reference pressure	[-]
f_v	Mass fraction of the vapor	[-]
k	Turbulent Kinetic Energy	[J/kg]
n	Pump speed	[rad/s]
$\vec{n}$	Surface normal	[-]
NCG_{tot}	Total non-condensable gas mass fraction	[-]
p	Pressure	[Pa]
p_v	Phase-change threshold pressure	[Pa]
$p_{f_{d,equil\,ref}}$	Reference pressure for the dissolved gas equilibrium mass fraction	[Pa]

Q_{ref}	Reference flow rate	[L/min]
R_e	Vapor generation rate	[-]
R_c	Vapor condensation rate	[-]
S_{fd}	Source of dissolved NCG	[kg/m^3]
$\vec{v}$	Fluid velocity vector	[m/s]
v_σ	Fluid velocity vector	[m/s]

Greek letter	***Description***	***Unit***
μ_t	Turbulent viscosity	[Pa·s]
ρ	Density of mixture	[kg/m^3]
ρ_g	Density of gas	[kg/m^3]
ρ_l	Density of liquid	[kg/m^3]
ρ_v	Density of vapor	[kg/m^3]
σ	Surface of control volume	[m^2]
Ω	Control volume	[m^3]
σ_f	Turbulent Schmidt number	[-]
σ_l	Surface tension	[N/m]

7. REFERENCES

[1] Heisler, A.S., Moskwa, J.J., Fronczak, F.J. "Simulated Helical Gear Pump Analysis Using a New CFD Approach." Proceedings of the ASME 2009 Fluids Engineering Division Summer Meeting. Volume 1: Symposia, Parts A, B and C. Vail, Colorado, USA. August 2–6, 2009. pp. 445-455. ASME. https://doi.org/10.1115/FEDSM2009-78472.

[2] Zhao, X., Vacca, A., Dhar, S. "Numerical Modeling of a Helical External Gear Pump With Continuous-Contact Gear Profile: A Comparison Between a Lumped-Parameter and a 3D CFD Approach of Simulation." Proceedings of the BATH/ASME 2018 Symposium on Fluid Power and Motion Control. BATH/ASME 2018 Symposium on Fluid Power and Motion Control. Bath, UK. September 12–14, 2018. V001T01A053. ASME. https://doi.org/10.1115/FPMC2018-8903.

[3] Pellegri, M., Vacca, A., Frosina, E., Buono, D., Senatore, A. Numerical analysis and experimental validation of Gerotor pumps: A comparison between a lumped parameter and a computational fluid dynamics-based approach. Proceedings of the Institution of Mechanical Engineers, Part C: Journal of Mechanical Engineering Science. 2017;231(23):4413-4430. https://doi.org/10.1177/0954406216666874.

[4] Frosina, E., Senatore, A., Buono, D., Stelson, K.A., Wang, F., Mohanty, B., Gust, M.J. "Vane Pump Power Split Transmission: Three Dimensional Computational Fluid Dynamics Modeling." Proceedings of the ASME/BATH 2015 Symposium on Fluid Power and Motion Control. ASME/BATH 2015 Symposium on Fluid Power and Motion Control. Chicago, Illinois, USA. October 12–14, 2015. V001T01A011. ASME. https://doi.org/10.1115/FPMC2015-9518.

[5] Borghi, M., Zardin, B. "Axial Balance of External Gear Pumps and Motors: Modelling and Discussing the Influence of Elastohydrodynamic Lubrication in the Axial Gap." Advances in Multidisciplinary Engineering. Ed. Jahanmir, S, Saka, N, Tucker, C, & Kim, S. ASME Press, 2016. https://doi.org/10.1115/1.861080_ch8.

[6] Schleihs, C., Viennet, E., Deeken, M., Ding, H., Xia, X., Lowry, S., Murrenhoff, H. 3D-CFD simulation of an axial piston displacement unit. In Proceedings of the 9th International Fluid Power Conference, Aachen, Germany, 24–26 March 2014; pp. 332–343.

[7] Zhou, J., Vacca, A., Casoli, P. A novel approach for predicting the operation of external gear pumps under cavitating conditions, Simulation Modelling Practice and Theory, Volume 45, 2014, Pages 35-49, ISSN 1569-190X, https://doi.org/10.1016/j.simpat.2014.03.009.

[8] Singhal, A. K., Athavale, M. M., Li, H., Jiang, Y. (August 19, 2002). "Mathematical Basis and Validation of the Full Cavitation Model ." ASME. J. Fluids Eng. September 2002; 124(3): 617–624. https://doi.org/10.1115/1.1486223.

[9] Simerics Inc. Simerics MP+'s User Manual - v 5.0.11; Simerics: Bellevue, WA, USA, 202

Biographies

Pietro Mazzei received his B.Sc and M.Sc of Mechanical Engineering degree at Federico II of Naples University, Italy in 2021. He received his Ph.D. degree on Industrial Engineering in 2023, focusing on the development of numerical models to analyze and optimize the performances and the noise emissions of external gear machines. Currently he is employed at CIRA (Centro Italiano Ricerche Aerospaziali) on the development of hybrid LTA vehicle as a pressure and thermal modeling expert.